SYNTHESIS, LUMINECENCE AND MAGNETIC PROPERTIES OF NANOCOMPOSITE MATERIALS BASED ON Mn:ZnSe/CdS/ZnS PARAMAGNETIC QUANTUM DOTS

Alisher Ishankulov[1,*], Kadriddin Khalilov[1], Serdar Özçelik[2], Yuriy Galyametdinov[3]
[1]Samarkand state university, Samarkand, Uzbekistan
[2]Izmir institute of technology, Izmir, Turkey
[3]Kazan National Research Technological University, Kazan, Russia
*Corresponding author: Ishankulov-alisher@mail.ru

ABSTRACT

Materials called triplet-structured ZnSe/CdS/ZnS quantum dots have recently become increasingly popular due to their highly efficient size-dependent luminescence in the entire visible range. Triplet quantum dots consist of a nanoparticle core that determines the wavelength of the radiation and a shell that acts as a passivator of surface states. This shell, in turn, allows the electron-hole pair to be localized in the core, which allows for increased luminescence efficiency. Quantum dots are superior to traditional phosphors in terms of photostability, have a narrow and intense emission peak, and also absorb light in a wide range. In order to make triplet-structured quantum dots exhibit magnetic properties, doping with Mn ions has been carried out. The size-dependent luminescence property and the relatively simple methods of their synthesis further increase scientific interest in them.

Keywords: ZnSe/CdS/ZnS, quantum dots, luminescence, nanocomposite, triplet, band gap.

INTRODUCTION

In recent decades, nanomaterials science has developed rapidly, leading to revolutionary advances in many areas of science and technology. Semiconductor nanocrystals or quantum dots (QDs) have attracted particular attention due to their unique optical and electronic properties, which can be tuned in a size-dependent manner through quantum confinement effects [1,2]. Quantum dots have been widely used in fields such as optoelectronics, biosignatures, solar energy, and quantum computing, especially due to their high photostability, narrow and intense luminescence peak, and wide absorption band [3,4].

To further expand the functional capabilities of quantum dots, it is important to simultaneously control the optical and magnetic properties of the materials. “Multimodal” or “bifunctional” nanomaterials that combine these two functions, such as magneto-optical quantum dots, have great potential for the development of new-generation diagnostics and therapeutics, as well as advanced electronic devices [5,6]. Doping with transition metal ions, in particular manganese (Mn^{2+}) ions, is an effective way to simultaneously control the optical and magnetic properties of semiconductor quantum dots. Mn^{2+} ions not only change the luminescence properties of quantum dots (for example, its time and wavelength), but also give them paramagnetic properties, which allows them to be manipulated under the influence of a magnetic field [7, 8].

The synthesis of “core\shell” and core\shell\shell structures allows passivation of defects on the surface of the core, increasing the luminescence quantum efficiency and improving the stability of nanocrystals [9, 10]. The ZnSe core is a semiconductor with a wide energy band gap, allowing emission in the mid-visible range. As an intermediate shell, CdS has a lattice constant matching the core, acts as an energy barrier and enhances the luminescence of Mn^{2+} ions in the core. The ZnS outer shell protects the core\shell system, further increasing the emission efficiency and protecting it from environmental influences [11, 12]. The synthesis of such complex heterostructures allows optimizing the effect of Mn^{2+} in the core and fine-tuning the properties of the final material.

The synthesis of nanocomposite materials with a complex core\shell\shell structure based on Mn:ZnSe quantum dots (Mn:ZnSe/CdS/ZnS) and the systematic study of their simultaneous optical and magnetic properties are of great scientific and practical importance. Although simpler core\shell structures based on Mn-doped ZnSe have been widely studied in the existing literature, the combined effect of CdS and ZnS shells, especially their effect on magnetic and luminescent properties, has not been sufficiently analyzed. The aim of this work is to successfully synthesize nanocomposite materials based on Mn:ZnSe/CdS/ZnS paramagnetic quantum dots, and to comprehensively study their morphological, structural, optical (luminescent) and magnetic properties. It is also aimed to determine the effect of the Mn^{2+} ion concentration and the thickness of the shell layers on the luminescent and magnetic properties of quantum dots.

LITERATURE REVIEW

Group II-VI quantum dots such as ZnSe, CdS, and ZnS have high stability and wide band gaps, and ZnSe QDs are promising for bioimaging and luminescent devices. However, to improve the low quantum efficiency and fast-decaying luminescence of pure ZnSe QDs, doping them with manganese (Mn^{2+}) ions is an effective strategy, as Mn^{2+} ions impart novel optical and magnetic properties, as well as paramagnetic properties that are used in spintronic and magnetic resonance imaging. The creation of core-shell structures is an effective way to enhance the luminescence efficiency, in which shell materials such as CdS and ZnS passivate defects and improve the quantum efficiency. Triple-shell nanocomposites such as Mn:ZnSe/CdS/ZnS have great potential for simultaneous control of optical and magnetic properties, opening new opportunities for multimodal imaging, spintronic devices, and sensors. This work aims to comprehensively study the morphological, structural, optical, and magnetic properties of Mn:ZnSe/CdS/ZnS structures, which will serve to optimize them for future practical applications.

METHODOLOGY

The following chemical reagents were used in the synthesis process: Zinc (Zn) source: Zinc acetate dihydrate ($Zn(CH_3COO)_3 \cdot 2H_2O$, 99.99%, Sigma-Aldrich). Selenium (Se) source: Selenium powder (Se, 99.999%, Sigma-Aldrich) dissolved in trioctylphosphine (TOP, 90%, Sigma-Aldrich) solvent (TOP-Se precursor) or bis(trimethylsilyl)selenide ($(TMS)_2Se$, 97%, Sigma-Aldrich). Manganese (Mn) source: Manganese acetate tetrahydrate ($Mn(CH_3COO)_2 \cdot 4H_2O$, 99.99%, Sigma-Aldrich) or manganese (II) chloride ($MnCl_2$, 99.99%, Sigma-Aldrich). Cadmium (Cd) source: Cadmium acetate dihydrate ($Cd(CH3COO)_2 \cdot 2H_2O$, 99.99%, Sigma-Aldrich) or cadmium oxide (CdO, 99.99%, Sigma-Aldrich). Sulfur (S) source: Sulfur powder (S, 99.999%, Sigma-Aldrich) dissolved in trioctylphosphine (TOP, 90%, Sigma-Aldrich) solvent (TOP-S precursor). Solvents and ligands: 1-Octadecene (ODE, 90%, Sigma-Aldrich), oleylamine (OLA, 90%, Sigma-Aldrich), oleic acid (OA, 90%, Sigma-Aldrich). Solvents for cleaning: Methanol (99.8%, Merck), acetone (99.8%, Merck), toluene (99.8%, Merck).

The following equipment was used in the synthesis and characterization processes: Synthesis reactor: A three-necked glass flask, a magnetic stirrer, a heating magnetic stirrer with thermocouple-controlled temperature control, a condenser for high-temperature reactions, and the synthesis was carried out in an inert gas (argon or nitrogen) environment.

SYNTHESIS METHODOLOGY

Nanocomposite materials based on Mn:ZnSe/CdS/ZnS paramagnetic quantum dots were synthesized stepwise using a high-temperature thermal injection method. This method allows obtaining high-quality nanocrystals with uniform size and core/shell structure.

Mn-doped ZnSe cores were synthesized as follows: First, zinc acetate dihydrate ($Zn(CH_3COO)_2 \cdot 2H_2O$) and a certain amount of manganese acetate tetrahydrate ($Mn(CH_3COO)_2 \cdot 4H_2O$) were added to the 1-Octadecene solvent. To study the degree of doping, the Mn concentration was varied between 0.5%, 1%, 3% and 5% (in atomic percentage, relative to Zn). The mixture was placed in a three-necked glass flask and heated to 120-150°C under an

inert atmosphere (argon). At this temperature, oleylamine or oleic acid was added as a ligand, stirred until the metal salts were completely dissolved, and water and other volatile compounds were distilled off. Then, the temperature of the mixture was rapidly increased to 280-300°C. At this temperature, a previously prepared Se precursor (e.g., TOP-Se solution) was quickly injected into the reaction mixture in a single injection. The reaction was held at elevated temperature for 5–15 min, which allowed the growth and crystallization of Mn:ZnSe nuclei. After the reaction was complete, the heating source was turned off and the flask was cooled to room temperature. The synthesized nuclei were dissolved in toluene and purified by centrifugation several times with a methanol/acetone mixture. The final product was stored in a dark, inert atmosphere.

CdS shell growth. An in situ method was used to grow CdS shells on the surface of Mn:ZnSe cores: The purified Mn:ZnSe cores were placed in a three-necked flask with a certain amount of ODE and oleylamine. The mixture was heated to 120°C under an inert atmosphere, distilled, and then the temperature was increased to 220-240°C. At this temperature, the Cd precursor (e.g., Cd acetate in ODE) and the S precursor (e.g., TOP-S in ODE) were separately and slowly injected (e.g., using a syringe pump over 1-3 hours) into the reaction mixture. This ensured uniform and controlled growth of the shell. The reaction was maintained for 1-3 hours. The synthesized Mn:ZnSe/CdS quantum dots were purified by the method described above (toluene/methanol-acetone).

Growing ZnS shells. The growth of the ZnS outer shell on the surface of the CdS-capped Mn:ZnSe/CdS quantum dots was also performed in situ: The purified Mn:ZnSe/CdS quantum dots were placed in a reaction flask together with ODE and oleylamine. The mixture was heated to 120°C under an inert atmosphere, distilled, and then the temperature was increased to 200–220°C. At this temperature, the Zn precursor (e.g., Zn acetate in ODE) and the S precursor (e.g., TOP-S in ODE) were separately and slowly (over 1–3 h) added to the reaction mixture. The reaction was continued for 1–3 h. The final Mn:ZnSe/CdS/ZnS nanocomposite quantum dots were dissolved in toluene and purified by several precipitation-centrifugation methods with a methanol/acetone mixture. The cleaned samples were dried in a vacuum drying cabinet at 40°C until morning and then stored in the dark, protected from moisture, and under an inert atmosphere for further analysis.

RESULTS DISCUSSION

This study schematically illustrates the synthesis mechanism and changes in optical properties of ZnSe quantum dots initially doped with Mn^{2+} (Mn:ZnSe) and their core/shell structures covered with CdS shells (Mn:ZnSe/CdS). The analysis results allow us to explain the synthesis process and photoluminescence properties in a coherent manner (Figure 1).

Mn:ZnSe cores were synthesized in aqueous medium under an inert nitrogen (N_2) atmosphere. In the reaction medium, Zn^{2+} and Mn^{2+} ions were used as metal cation sources, and NaHSe was used as a selenium source. L-cysteine molecules act as ligands and surface passivators, binding to the surface of quantum dots via thiol (–SH) groups. This prevents agglomeration of the resulting particles, ensures their stability in water, and a colloidal state. The reaction was carried out for about 3 hours under highly alkaline conditions (pH ≈ 10), resulting in the formation of Mn:ZnSe cores, in which Mn^{2+} ions are internally incorporated into the ZnSe crystal lattice. At this stage, Mn^{2+} ions are formed as the main luminescent center. In the next step, a CdS shell is grown around the Mn:ZnSe cores. The shell formation process is carried out under ultraviolet radiation with a wavelength of 365 nm. The UV-induced conditions allow for relatively uniform and controlled shell growth, resulting in Mn:ZnSe/CdS core/shell hybrid quantum dots, with L-cysteine molecules continuing to passivate the outer surface.

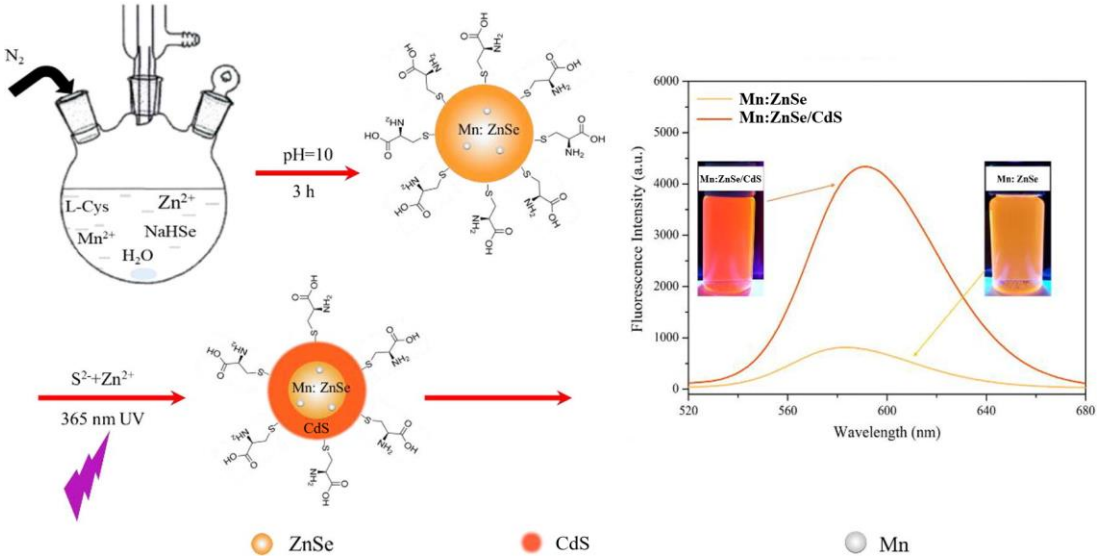

Figure 1. Schematic representation of the synthesis mechanism and changes in optical properties of Mn^{2+}-doped ZnSe quantum dots (Mn:ZnSe) and their core/shell structures covered with a CdS shell (Mn:ZnSe/CdS).

The photoluminescence spectrum of Mn:ZnSe cores exhibits an emission peak at approximately 590 nm. This emission is associated with the spin-forbidden internal $^4T_1 \rightarrow {}^6A_1$ transitions characteristic of Mn^{2+} ions and is usually observed in the yellow–orange spectral region. However, due to the defects and surface traps present on the surface of the cores, the intensity of this emission is relatively low. After the CdS shell is grown, the position of the emission peak in the PL spectrum of Mn:ZnSe/CdS quantum dots does not change much and remains around 590 nm. This indicates that it is the Mn^{2+} ions that are active as the luminescence center and that their energy levels do not change significantly with the formation of the shell. At the same time, the emission intensity increases by about 5–6 times, which confirms that the CdS shell effectively passivates the surface defects. This difference is also clearly visible in visual observations: while the Mn:ZnSe sample luminescences in a relatively weak orange color under UV light, the Mn:ZnSe/CdS sample exhibits a much brighter, more intense orange–red luminescence. This result indicates a significant increase in quantum efficiency. The main function of the CdS shell is to eliminate non-radiative recombination centers on the surface of the Mn:ZnSe cores. The shell protects excitons from loss to surface states and allows their energy to be efficiently transferred to the Mn^{2+} ions. As a result, the probability of radiative recombination increases and the emission characteristic of Mn^{2+} is enhanced. Importantly, the almost constant emission wavelength indicates that the Mn^{2+} ions are located on the surface of the core and that the CdS shell plays only a passivating role. This is strong evidence for the successful formation of the core/shell structure.

The photoluminescence (PL) spectra of Mn^{2+}-doped ZnSe quantum dots with different shell structures, namely Mn:ZnSe/CdS and Mn/ZnSe/CdS/ZnS structures, measured at room temperature under the same excitation conditions are presented (Fig. 2). Clear differences in the spectral positions and widths of the emission peaks are observed, which is important in characterizing the optical properties of the shell-structured Mn^{2+} luminescent centers. A broad emission band is observed in the range of approximately 600–620 nm for the Mn:ZnSe/CdS sample. This emission is associated with the spin-forbidden internal transition ($^4T_1 \rightarrow {}^6A_1$) characteristic of Mn^{2+} ions and is usually observed in the orange region of the spectrum. The relatively large full width at half maximum (FWHM) indicates a significant non-uniform broadening of the emission. This is explained by the differentiation of the local crystal field around the Mn^{2+} ions and the preservation of surface-related radiative recombination pathways. The presence of only one ZnS shell layer cannot completely passivate the traps on the surface of the

ZnSe core, as a result of which some of the excitons are trapped in surface states before energy is transferred to the Mn^{2+} centers.

In contrast, Mn:ZnSe/CdS/ZnS quantum dots exhibit a much narrower PL peak around 540–560 nm and a significant blue shift compared to the Mn:ZnSe/CdS sample. The narrowing of the emission width indicates improved structural uniformity of the core and a more uniform distribution of Mn^{2+} ions. The intermediate CdS shell and the ZnS outer shell on top of it effectively passivate surface defects and reduce the deformation caused by lattice mismatch. As a result, the radiative recombination through surface traps is significantly weakened and the emission characteristic of Mn^{2+} ions is more pronounced. The blue shift observed in the Mn:ZnSe/CdS/ZnS structure is explained by the change in the local crystal field around the Mn^{2+} ions due to the multilayer shell configuration. The enhanced quantum confinement and reduced surface effects change the energy levels of Mn^{2+} ions, leading to a shift in emission to shorter wavelengths. In addition, thermal annealing during the shell growth process further improves the crystal quality and structural uniformity of the cores, as evidenced by the absence of additional defect emission bands in the PL spectra.

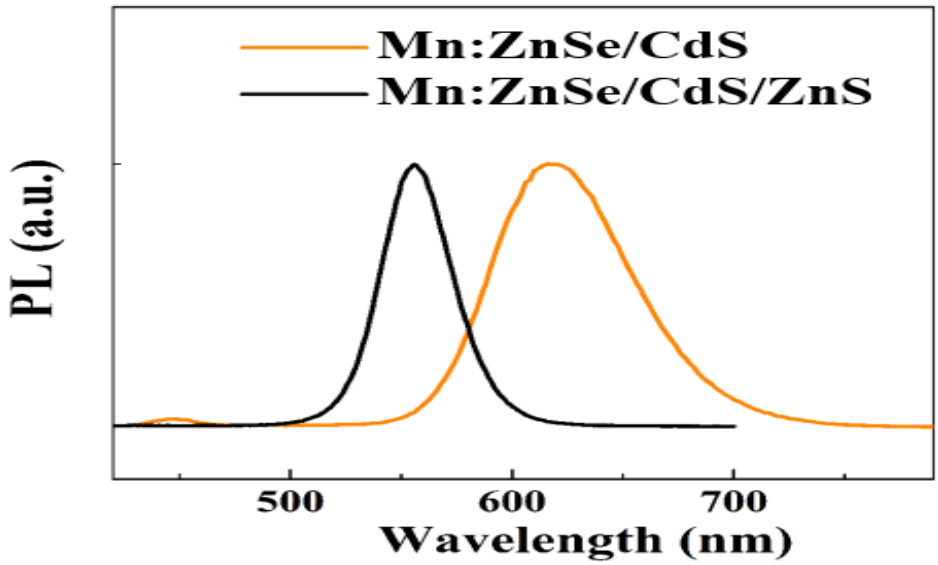

Figure 2. Luminescence spectra of Mn:ZnSe/CdS and Mn:ZnSe/CdS/ZnS quantum dots.

The normalized steady-state photoluminescence spectra of Mn^{2+}-undoped ZnSe/CdS/ZnS and Mn^{2+}-doped ZnSe/CdS/ZnS quantum dots are presented (Fig. 3). Both spectra were measured under the same excitation conditions, allowing a direct comparison of the shape, location, and width of the emission peaks due to the normalization of the intensities. The Mn^{2+}-undoped ZnSe/CdS/ZnS sample exhibits a narrow and symmetric emission peak located around 540–550 nm. This emission is associated with radiative recombination of excitons in the ZnSe core, indicating effective passivation of surface defects by the multilayer CdS/ZnS shell. The narrowness of the spectrum and the absence of additional emission bands indicate a high crystalline quality of the core and a significant suppression of radiative recombination channels.

In Mn^{2+}-doped ZnSe/CdS/ZnS quantum dots, the emission peak is slightly shifted to longer wavelengths (approximately 5–10 nm), while the spectral shape and width remain almost unchanged. This small redshift is explained by the change in the local crystal field and weak deformations in the lattice as a result of the introduction of Mn^{2+} ions into the core. At the same time, the narrow and symmetrical spectrum indicates that the Mn^{2+} ions are evenly distributed and that no new surface or deep energy trap states are formed. Importantly, the distinct yellow–orange emission band (~600 nm) due to the $^4T_1 \rightarrow {}^6A_1$ transition characteristic of Mn^{2+} ions is not observed. This indicates that the Mn^{2+} concentration is low and that the multilayer CdS/ZnS shell effectively optically separates the Mn^{2+} centers from excitons. As a result, the energy transfer

process does not compete with Mn^{2+} emission, and exciton recombination remains the dominant mechanism. Also, the almost overlapping of both spectra indicates that the CdS/ZnS shell structure effectively "screens" the negative effects of Mn^{2+} dopants. This confirms that the Mn^{2+} ions are internally doped, playing a role mainly in modifying the local electronic structure of the core, but do not degrade the optical quality.

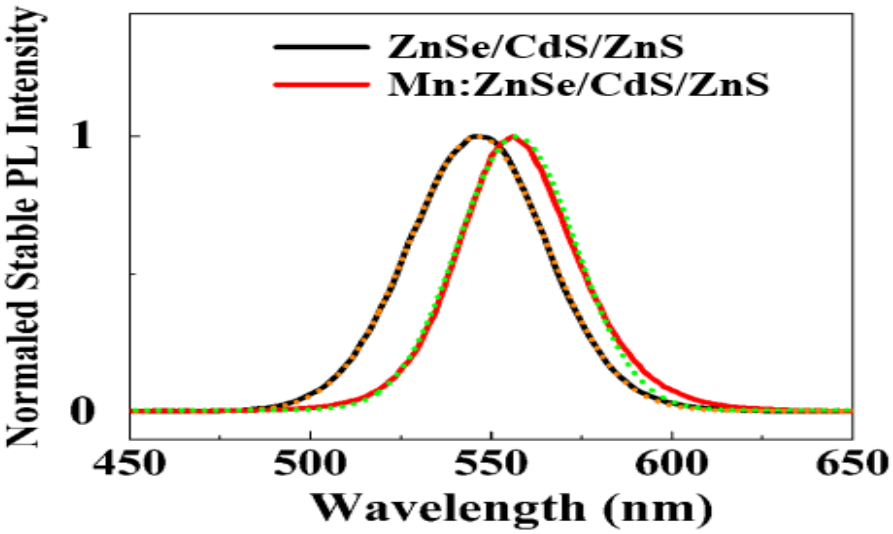

Figure 3. Luminescence spectra of Mn^{+2}-doped and undoped triplet ZnSe/CdS/ZnS quantum dots.

The study analyzed the structure, optical properties and luminescence kinetics of Mn-doped ZnSe-based quantum dots with a complex core/shell structure (Fig. 4). The analysis consists of three parts: a) structure and energy diagram, b) absorption and luminescence spectra, c) luminescence kinetics. This part shows a schematic representation of four different quantum dots

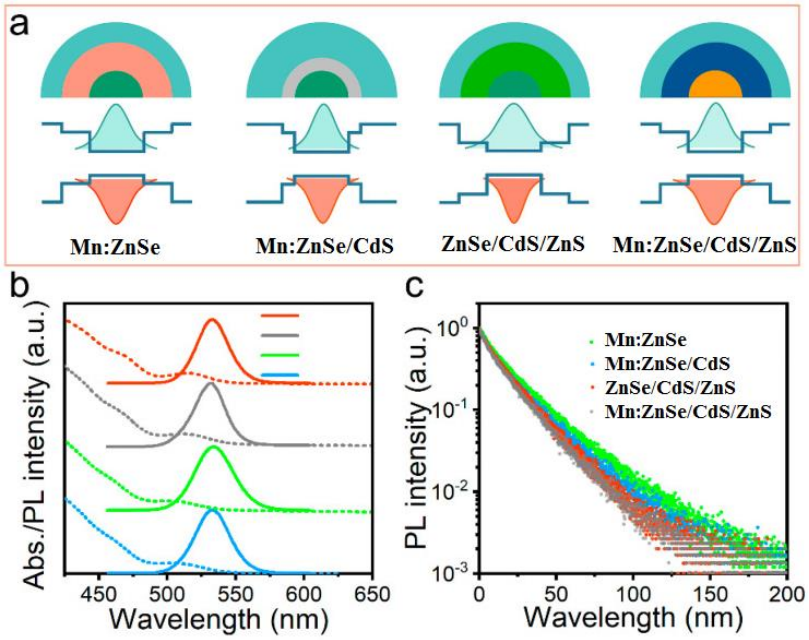

Figure 4. Morphological and optical properties of different quantum dots

and their approximate energy bands. This representation (Fig. 4) demonstrates the control of the optical properties of quantum dots by obtaining complex core/shell/shell structures. The main

conclusion is that the sequential addition of ZnS and CdS shells to the Mn:ZnSe core increases the luminescence quantum efficiency (b-graph, intensity increase), mainly through excitonic emission (green range). The luminescence decay kinetics, however, improves slightly with the addition of shells, confirming the effective passivation of surface defects.

We can see from the images of Mn:ZnSe, Mn:ZnSe/CdS, ZnSe/CdS/ZnS and Mn:ZnSe/CdS/ZnS quantum dots with different compositions that the structures clearly show a gradual change in the location of the energy bands. The addition of shell layers limits the escape of carriers into surface traps and ensures a more efficient localization of excitons in the core. In particular, the outer ZnS shell has a high energy band gap, which plays a strong passivation role (Fig. 4a). The absorption and photoluminescence spectra for the samples are presented (Fig. 4b). While the pure Mn:ZnSe sample has a relatively broad and low-intensity PL peak, the emission intensity increases significantly when CdS and ZnS shell layers are added. This is explained by the reduction of surface defects and the suppression of non-radiative recombination channels. The highest PL intensity is observed in the Mn:ZnSe/CdS/ZnS structure, which confirms the effective passivation of the multilayer shell. The shift of the spectra is associated with quantum confinement effects depending on the shell thickness and composition. The change in the PL intensity with wavelength is given on a logarithmic scale. In nanocrystals covered with multilayer shells, the PL decay occurs more slowly, i.e., their effective lifetime is longer. This result indicates that the interaction of carriers with surface states is reduced and the probability of radiative recombination is increased. The most stable and slow decay is observed for the Mn:ZnSe/CdS/ZnS sample (Fig. 4c).

CONCLUSIONS

These results show that the complexity of the core/shell structure (CdS and ZnS shells) dramatically changes the energy structure, energy transfer mechanisms, and luminescent properties of quantum dots. While Mn^{2+} emission is dominant in simple Mn:ZnSe cores, excitonic emission dominates in the multilayer Mn:ZnSe/CdS/ZnS system. This demonstrates the possibility of fine-tuning the luminescence mechanisms through shell engineering, making these systems very promising materials for optoelectronics, photonics, and bioluminescence. Overall, it is clear that the formation of multilayer (CdS/ZnS) shells in Mn-doped ZnSe nanocrystals significantly improves the optical properties, in particular, increases the photoluminescence intensity and stability.

ACKNOWLEDGEMENT

This work was supported by grant number 75/2024-PD allocated for the defense of doctoral dissertations, conducting scientific research work for young candidates of the Academy of Sciences of the Republic of Tatarstan, as well as for performing work functions in scientific and educational organizations of the Republic of Tatarstan within the framework of the State Program of the Republic of Tatarstan “Scientific and Technological Development of the Republic of Tatarstan”. We would like to thank the Kazan National Research Technological University and the Izmir Institute of Technology for their close assistance in obtaining the research results.

REFERENCES

1. Alshehri K. et al. Vacancy-driven improvement of optical and ferromagnetism in Co^{2+}/La^{3+} dual-doped ZnS quantum dots for spintronic and optoelectronic applications //Materials Science in Semiconductor Processing. – 2026. – T. 203. – P. 110243.
2. Williams A. G. et al. LaMer growth of iron nanoparticles for magnetic particle imaging //Academia Materials Science. – 2025. – P. 2. – №. 4.
3. Zhou Z. et al. High-Stability Thick-Shell CdZnSeS/CdZnS/ZnS Green-Alloy Quantum Dots in Photoluminescent Diffuser-Plate Masterbatches //Materials. – 2025. – T. 18. – №. 23. – P. 5383.

4. Huang W. Ji R., Wang K., Li J., Kim H. S., Wu C., Kim T. W. . Fluorescence Modulation Behavior of Quantum Dots under Alternating Electric Fields and Applications in Logic and Neuromorphic Computing //ACS Applied Materials & Interfaces. – 2025.
5. Cherni A. Zeiri N., Yahyaoui N., Hayrapetyan D. B., Murshed M. N. . Deep Learning-Assisted Prediction of Electric Field Impact on Impurity Photoionization Cross Section in CdS/ZnSe Core/Shell Spherical Quantum Dot embedded in PVA Matrix //Sensors and Actuators A: Physical. – 2025. – P. 117365.
6. Chacko A. R. Korah B. K., Narayanan R., Punnoose M. S., Joseph S., Mathew B. . Controllable synthesis of amino nitrogen dots for sustainable enantioselective and environmental chemical sensing applications //Journal of Environmental Chemical Engineering. – 2025. – P. 120509.
7. Yu C., Li S., Ning J. Enhanced Performance of Giant Power Exponent Superlinear Photodetectors Based on ZnS/MgS Core–Shell Quantum Dots //Laser & Photonics Reviews. – 2025. – P. e01328.
8. Sulaymonovich D. S., Fayzullaev N., Nazirova R., Ishankulov A., Omidi M., Al-Nuaimi B., Faraji, M. (2025). Single-atom silver-borophene hybrid hydrogels for electrically stimulated wound healing: a multifunctional antibacterial platform. Biomaterials Science, 13(15), P 4180-4198.
9. Yumashev A., Shichiyakh R., Ishankulov, A. (2025). Electrochemical biosensors for early detection of Alzheimer's disease. Clinica Chimica Acta, 120278.
10. Chang K. P. et al. Improved characteristics of CdSe/CdS/ZnS core-shell quantum dots using an oleylamine-modified process //Nanomaterials. – 2022. – Т. 12. – №. 6. – P. 909.
11. Ishankulov A. F. et al. Size-optical characteristics of CdSe/ZnS quantum dots modified by thiol stabilizers //Journal of Sol-Gel Science and Technology. – 2023. – Т. 108. – №. 2. – P. 292-297.
12. Zidan M. D. et al. Thermal lens investigation of the CdSe quantum dots using dual beam z-scan technique //Results in Optics. – 2024. – Т. 16. – P. 100692.